Accurate theory of excitons in GaAs-$Ga_{1-x}Al_xAs$ quantum wells

Lucio Claudio Andreani
Institut Romand de Recherche Numérique en Physique des Matériaux (IRRMA), PHB-Ecublens, CH-1015 Lausanne, Switzerland

Alfredo Pasquarello
Institut de Physique Théorique, Ecole Polytechnique Fédérale de Lausanne, PHB-Ecublens, CH-1015 Lausanne, Switzerland

(Received 7 May 1990)

Binding energies of excitons in quantum wells are calculated including valence-band mixing and also other important effects, namely Coulomb coupling between excitons belonging to different subbands (which is predominantly with the exciton continuum), nonparabolicity of the bulk conduction band, and the difference in dielectric constants between well and barrier materials. All these effects are found to be of a comparable size, tend to increase the binding energies, and taken together result in very high binding energies, particularly in narrow GaAs/AlAs quantum wells. Binding energies can be even higher than the two-dimensional limit of four times the bulk Rydberg. Theoretical results agree within a few tenths of a milli-electron-volt with available photoluminescence excitation experiments. Valence-band mixing gives a finite oscillator strength to some excitons not in s states, but does not change the selection rules based on parity. Calculated oscillator strengths of the ground-state heavy- and light-hole excitons are found to be in good agreement with absorption and reflectivity experiments.

I. INTRODUCTION

Excitons in semiconductor quantum wells (QW's) have been the subject of numerous investigations since the first observations by Dingle and co-workers.[1-3] Excitonic effects in GaAs-$Ga_{1-x}Al_xAs$ quantum wells grown by molecular-beam epitaxy are much more prominent than in bulk samples of comparable quality, both in absorption and in emission. The photoluminescence is often dominated by intrinsic emission,[4] and excitons are seen in optical spectra up to room temperature. Such properties can be partly understood as arising from the increase in binding energy and oscillator strength due to confinement of the carriers. Therefore an understanding of the effects which determine binding energies and oscillator strengths represents a basic piece of knowledge in this field.

The overall trends in these properties are determined by quantum confinement. Binding energies and oscillator strengths are first increased as the well width is reduced, due to the smaller electron-hole separation.[5,6] This holds as long as the exciton wave function remains confined in the well region: for narrow wells and finite barrier height, the wave function starts to leak into the barriers, making the binding energy decrease towards the value appropriate to the bulk barrier material.[7] However, besides the effect of quantum confinement, exciton binding energies and oscillator strengths are also affected by the fourfold degeneracy of the uppermost bulk valence band at the Γ point. In a QW, this degeneracy is removed, giving rise to heavy- and light-hole states (HH,LH): heavy and light holes are mixed at finite values of the in-plane vector $\mathbf{k}_{\|}$,[8,9] giving rise to strong nonparabolicities in the space-quantized valence-band structure. These features occur at the same scale of $\mathbf{k}_{\|}$ vectors relevant for the construction of exciton states, and must therefore be taken into account for the exciton problem.

Existing theories of quantum-well excitons can be classified according to whether they neglect valence-band mixing[5-7,10-13] or include it.[14-22] There is general agreement that valence-band mixing increases the binding energy and the oscillator strength of the ground-state HH and LH excitons. However, even restricting oneselves to the works that include valence-band mixing, published results for exciton binding energies show a considerable spread of values. This is due to various reasons. First, some previous treatments of valence-band mixing[14,16,19] neglected the correct symmetry properties of the exciton envelope function. This resulted in an inaccurate evaluation of exciton binding energies, as well as in incorrect selection rules for optical transitions. Second, in addition to valence-band mixing, there are other effects which can significantly alter the exciton binding energy: these are Coulomb coupling between excitons belonging to different subbands,[18,21,22] nonparabolicity of the bulk conduction band,[18,22] and the difference in dielectric constants between well and barrier materials.[12,13] Each single effect has already been studied, but no theory exists which takes into account all of them together, although these effects can be of a comparable size. Third, even

when Coulomb coupling is included, an additional difficulty arises for excitons which are degenerate with the continuum of other exciton series. Coupling with the continuum is particularly difficult to include, but is also particularly sizeable.

Our main point here is that all the effects mentioned above go in the direction of increasing the binding energy, at least for the ground-state HH and LH excitons in GaAs-$Ga_{1-x}Al_xAs$ quantum wells. Hence their combination can yield significantly higher binding energies than in any of the existent theories.

This work is devoted to an accurate calculation of binding energies and oscillator strengths for ground- and excited-state excitons in [001]-grown type-I quantum wells. In Sec. II we describe the theoretical framework. We give particular emphasis to the points (selection rules for excitonic transitions, the treatment of nonparabolicity, the effect of the dielectric mismatch, coupling with the continuum) which are sometimes controversial in the existing literature. In Sec. III we present results for binding energies, and in Sec. IV for the oscillator strengths. Section V contains concluding remarks. Numerical results are obtained for GaAs-$Ga_{1-x}Al_xAs$ quantum wells, but the theory could be applied to other III-V structures. Comparison with experiment is emphasized throughout. The results obtained with this theory were first published in Ref. 22, but without the effect of the dielectric mismatch.

II. THEORY

A. Expansion of the exciton wave function

The theory of quantum-confined excitons is based on the effective-mass approximation in the envelope-function scheme.[23] In this scheme, the difference in the band edge between well and barrier materials is regarded as an effective potential for the carriers, which gives rise to quantized subbands. The envelope-function is required to satisfy current-conserving boundary conditions at the interface.[23] Detailed investigations[24] indicate that this scheme is quite appropriate for GaAs-$Ga_{1-x}Al_xAs$ heterostructures. Experience shows that predictions of the envelope function theory often maintain quantitative validity down to well widths of the order of 20 Å.[25,26] The situation is likely to be more favorable for the exciton problem, at least in type-I quantum wells, since the electron-hole interaction tends to confine the exciton within the well and an inaccurate treatment of the interface region is of little concern. Inaccurate predictions for narrow wells are likely to be due to the parameters of the theory, which are strongly renormalized for energies far from the band edge, rather than to a breakdown of the theory in itself.

We take the z axis as the growth direction. The exciton Hamiltonian in the effective-mass approximation is a 4×4 matrix operator given by

$$\begin{aligned} H_{ss'} = {} & E_c(-i\nabla_e)\delta_{ss'} + T_{ss'}(-i\nabla_h) \\ & + [V_e(z_e) + V_h(z_h)]\delta_{ss'} \\ & + [V_C(\mathbf{r}_e - \mathbf{r}_h) + V_{\rm im}(\mathbf{r}_e, \mathbf{r}_h)]\delta_{ss'}, \end{aligned} \tag{1}$$

where $E_c(\mathbf{k})$ is the nonparabolic conduction-band dispersion (see below), $T_{ss'}(\mathbf{k})$ is the Luttinger Hamiltonian,[27] V_e, V_h are square-well confinement potentials for electrons and holes, $V_C(\mathbf{r}) = -e^2/(\epsilon|\mathbf{r}|)$ is the electron-hole Coulomb potential screened by the low-frequency dielectric constant ε of the well material, and $V_{\rm im}(\mathbf{r}_e, \mathbf{r}_h)$ represents the potential due to all image charges. An explicit expression for $V_C + V_{\rm im}$ is given in Ref. 28 for the analogous case of acceptor impurities.

We do not consider the spin of the conduction band, and therefore neglect the electron-hole exchange interaction. The spin index $s = \frac{3}{2}, \frac{1}{2}, -\frac{1}{2}, -\frac{3}{2}$ corresponds to the angular momentum $\frac{3}{2}$ of the uppermost Γ_8 valence band at the Γ point. Remote bands are not explicitly considered, but their effect is included in the band parameters up to second order. The exciton envelope function is a four-component spinor labeled by the index s. For zero exciton wave vector, we represent it as

$$\begin{aligned} F^s(\rho, \theta, z_e, z_h) = \sum_{ij} \int \frac{d\mathbf{k}_\parallel}{(2\pi)^{3/2}} G_{ij}(\mathbf{k}_\parallel) e^{i\mathbf{k}_\parallel \cdot \rho} \\ \times c_i(z_e) v^s_{j\mathbf{k}_\parallel}(z_h), \end{aligned} \tag{2}$$

where $\mathbf{k}_\parallel = (k_\parallel, \alpha)$ is the Bloch vector of the subbands, $\boldsymbol{\rho} = (\rho, \theta)$ is the relative coordinate in the xy plane, $c_i(z_e), v_{j\mathbf{k}_\parallel}(z_h)$ are envelope functions of conduction and valence subbands, the index i (j) denotes the principal quantum number of conduction (valence) subbands, and $G_{ij}(\mathbf{k}_\parallel)$ is the in-plane wave function in k space.

In the Luttinger Hamiltonian, we neglect the small $\mathbf{k}$ linear terms arising from the lack of inversion symmetry of the zinc-blende lattice. We also adopt the axial approximation,[9] as warping of the valence subbands has been found to have a very small effect on the exciton binding energy:[21] in this approximation, the exciton problem acquires cylindrical symmetry around the growth direction. The transformation properties of the valence envelope functions under rotations in the k_x-k_y plane can be found by applying the rotation operator $\exp(-i\alpha J_z)$,[29] and are

$$v^s_{(k_\parallel,\alpha)}(z) = e^{-is\alpha} v^s_{(k_\parallel,0)}(z). \tag{3}$$

It is important to observe that, even if the dispersion of the valence subbands is taken to be axially symmetric, the spin components of the valence envelope function depend on the direction of $\mathbf{k}_\parallel$ in the k_x-k_y plane according to Eq. (3). This fact was apparently missed in some previous investigations.[14,16,19] Omitting the phase factor $\exp(-is\alpha)$ results in an overestimation of binding energies, and in selection rules inconsistent with symmetry properties, as already discussed.[20,22]

From these transformation properties, it can be shown

that the in-plane wave function $G_{ij}(\mathbf{k}_\parallel)$ can be taken of the form

$$G_{ij}(\mathbf{k}_\parallel) = g_{ij}(k_\parallel)e^{im\alpha}, \tag{4}$$

where m is a conserved quantum number which can be interpreted as the projection of the total angular momentum along the growth direction. The angular dependence of the exciton envelope function (2) can be found by inserting (3) into (2) and performing the angular integration, which gives

$$F^s(\rho,\theta,z_e,z_h) = i^{m-s}e^{i(m-s)\theta} \times \sum_{ij}\int \frac{k_\parallel\, dk_\parallel}{(2\pi)^{1/2}} g_{ij}(k_\parallel)c_i(z_e) \times v^s_{jk_\parallel}(z_h)J_{m-s}(k_\parallel\rho), \tag{5}$$

where J_{m-s} are Bessel functions and we write for simplicity $v^s_{jk_\parallel}(z)$ instead of $v^s_{j(k_\parallel,0)}(z)$. Equation (5) shows that different spin components of the exciton envelope function have different values of the orbital angular momentum $l = m - s$. Moreover, a spin component with orbital angular momentum l behaves like ρ^l for small ρ. We do not insist on these symmetry properties, as they have already been discussed in detail in the literature.[15,20,22,28]

We neglect coupling between different conduction subbands, which are well separated in energy. In this approximation, spin-degenerate valence subbands are not coupled by the Coulomb potential, and only one of them needs to be included in the expansion (2). We choose to work with valence envelope functions such that the components $\frac{3}{2},-\frac{1}{2}$ are even in z, and the components $\frac{1}{2},-\frac{3}{2}$ are odd[29] (our convention is opposite to that of Ref. 20). Kramers-degenerate excitons can be found by considering time-reversed valence states, and by letting $m \to -m$. Considering also the electron spin, each exciton state is fourfold degenerate in the neglect of the exchange interaction.

In this formalism, excitons are classified by two quantum numbers: the index i of the conduction subband, and the z projection of the total angular momentum, which we have called m. Trial states belonging to different valence subbands, but with the same value of m, are coupled by the Coulomb interaction. If an exciton originates largely from a particular valence subband, it is possible to relate the quantum number m to the ones which are usually employed: s,p,d states, ... Let s_0 be the spin component which is nonvanishing in the neglect of valence band mixing. s-states have zero orbital angular momentum for that component and correspond to $m = s_0$, p states correspond to $m = s_0 \pm 1$, and so on. Note that there are two $2p$ states, and they are not degenerate in the presence of valence-band mixing, because they correspond to different values of m: we denote them by p_+ and p_-. The approximate relation between the quantum number m and the orbital symmetries of the exciton is illustrated in Table I for four different hole levels. For example, the ground-state LH1-CB1 exciton couples to d_- states of the HH1-CB1 exciton, and to p_+ states of the HH2-CB1 exciton. Ground-state excitons couple with each other only when the corresponding subbands have the same symmetry, for example HH1-CB1 and HH3-CB1.

TABLE I. Relation between the quantum number m and the usual quantum numbers (s,p,d states ...).

hole level	Values of m for different symmetries				
	d_-	p_-	s	p_+	d_+
HH1	$-\frac{1}{2}$	$\frac{1}{2}$	$\frac{3}{2}$	$\frac{5}{2}$	$\frac{7}{2}$
LH2	$-\frac{3}{2}$	$-\frac{1}{2}$	$\frac{1}{2}$	$\frac{3}{2}$	$\frac{5}{2}$
LH1	$-\frac{5}{2}$	$-\frac{3}{2}$	$-\frac{1}{2}$	$\frac{1}{2}$	$\frac{3}{2}$
HH2	$-\frac{7}{2}$	$-\frac{5}{2}$	$-\frac{3}{2}$	$-\frac{1}{2}$	$\frac{1}{2}$

B. Computational details

In order to find exciton levels, the radial function $g_{ij}(k_\parallel)$ is expanded into a nonorthogonal basis,

$$g_{ij}(k_\parallel) = \sum_\nu a_{ij\nu}h_\nu(k_\parallel). \tag{6}$$

The basis functions $h_\nu(k_\parallel)$ consist of two-dimensional hydrogenic wave functions of the $1s$ state, which are decreasing exponentials in ρ space, and which in k space have the form

$$h_\nu(k_\parallel) = \frac{2\alpha_\nu^2}{(k_\parallel^2+\alpha_\nu^2)^{3/2}}. \tag{7}$$

The parameters α_ν are chosen in geometrical progression centered around the inverse exciton radius. We also include in the basis set some Gaussians in $\mathbf{k}_\parallel$ space:

$$h_\nu(k_\parallel) = e^{-(k_\parallel-k_\nu)^2/(2\sigma^2)}. \tag{8}$$

For a small width σ, states (8) describe delocalized states in ρ space, and are well suited in order to represent states of the exciton continuum (this point is discussed in more detail below).

Exciton eigenenergies and eigenfunctions are obtained by taking Hamiltonian and overlap matrix elements within the above basis and by solving a generalized eigenvalue equation for the expansion coefficients. The matrix elements of the kinetic part of the Hamiltonian have the form

$$\langle ij\nu|E_c + T_{ss'} + V_e + V_h|ij'\nu'\rangle = \int_0^\infty k_\parallel\, dk_\parallel\, [E_{ci}(k_\parallel) - E_{vj}(k_\parallel)]h_\nu(k_\parallel)h_{\nu'}(k_\parallel)\delta_{jj'}, \tag{9}$$

where $E_{vj}(k_\parallel)$ contains the complicated dispersion of the valence subbands due to HH-LH mixing. The matrix elements of the Coulomb potential have the form

$$\langle ij\nu|V_C|ij'\nu'\rangle = \int_0^{2\pi} d\theta \int_0^\infty k_\parallel\, dk_\parallel \int_0^\infty k'_\parallel\, dk'_\parallel\, h_\nu(k_\parallel)h_{\nu'}(k'_\parallel)V(ijk_\parallel, ij'k'_\parallel;\theta;m), \tag{10}$$

where

$$V(ijk_\parallel, ij'k'_\parallel;\theta;m) = -\frac{e^2}{2\pi\varepsilon}\frac{1}{|\mathbf{k}_\parallel - \mathbf{k}'_\parallel|}\sum_s e^{i(m-s)\theta}\iint dz_e\, dz_h\, |c_i(z_e)|^2 v^s_{jk_\parallel}(z_h)^* v^s_{j'k'_\parallel}(z_h) e^{-|\mathbf{k}_\parallel - \mathbf{k}'_\parallel||z_e - z_h|}. \tag{11}$$

Here $\theta = \alpha - \alpha'$ is the angle between $\mathbf{k}_\parallel$ and $\mathbf{k}'_\parallel$. Note that the contribution of different spin components is weighted with the factor $e^{i(m-s)\theta}$ in the θ integral: this tends to suppress the contribution of spin components with orbital angular momentum $l \neq 0$.

An important feature of the k-space Coulomb potential (11) is that the exponential factor $\exp[-|\mathbf{k}_\parallel - \mathbf{k}'_\parallel||z_e - z_h|]$ is piecewise separable in the electron and hole coordinates. Using the explicit form for the valence envelope functions given in Ref. 29, we see that the $dz_e\, dz_h$ integral in Eq. (11) reduces to products of one-dimensional integrals which involve combinations of trigonometric and exponential functions. Hence (11) can be evaluated analytically, although with a lengthy algebra. This represents a major simplification in numerical calculations, and is also a distinct virtue of the present theory, because it allows an analytical treatment of current-conserving boundary conditions and different band parameters in well and barrier materials. Moreover, the matrix elements of the image charge potential also depend exponentially on z_e, z_h, so that the contribution of all image charges reduces to a geometrical series which can be summed analytically.[28,30] The remaining three-dimensional integral over $k_\parallel, k'_\parallel$ and θ is done numerically by Gaussian integration. A technical problem has to be solved, since the argument of the θ integral in (9) is logarithmically divergent near $\theta = 0$, although the integral itself is finite. We add and subtract a function which removes the singularity, but which is sufficiently simple to be integrated by hand.

The expansion in a large basis set allows us to control convergence both in the number of subbands and in the number of trial functions. The number of valence subbands included in the expansion is usually two or three: the expansion set is smaller than in Ref. 21, as here the basis already contains valence-band mixing. Numerical convergence is better than 0.2 meV in the range of well widths considered here (GaAs-$Ga_{1-x}Al_xAs$ quantum wells with L ranging from 30 to 200 Å).

C. Oscillator strength

The oscillator strength is a dimensionless quantity, which for excitons in quantum wells is proportional to the area of the sample. The relevant quantity is thus the oscillator strength per unit area, which in the effective-mass approximation is calculated to be

$$\tilde{f} = \frac{2}{m_0 E_g}\left|\sum_s \langle u_c|\boldsymbol{\varepsilon}\cdot\mathbf{p}|u^s_v\rangle \times \sum_{j\nu} a_{ij\nu}\int \frac{d\mathbf{k}_\parallel}{(2\pi)^{3/2}} h_\nu(k_\parallel) \times e^{i(m-s)\alpha} I^s_{ij}(k_\parallel)\right|^2, \tag{12}$$

where u_c, u_v are Bloch functions of conduction and valence bands at $\mathbf{k} = 0$, and

$$I^s_{ij}(k_\parallel) = \int dz\, c_i(z) v^s_{jk_\parallel}(z) \tag{13}$$

is the overlap integral between envelope functions of conduction and valence subbands. Expression (12) must be summed over the fourfold-degenerate excitons.

Different kinds of selection rules come from the integral over the angle α of $\mathbf{k}_\parallel$, from the momentum matrix element between Bloch functions, and from the overlap integral (13). The integral over α is nonzero only for $s = m$, hence at most one spin component can be optically active, i.e., the one with zero orbital angular momentum. Note that a spin component with $l = 0$ exists only for states with $|m| \leq \frac{3}{2}$, and states with $|m| > \frac{3}{2}$ are forbidden in the axial approximation. But even when there exists a spin component such that $s = m$, the oscillator strength vanishes when $\langle u_c|\boldsymbol{\varepsilon}\cdot\mathbf{p}|u^s_v\rangle = 0$, or when conduction and valence states in (13) have opposite parities. The resulting selection rules are summarized in Table II (where, for completeness, we consider also the case of two-photon transitions[31]) for excitons with $|m| \leq \frac{3}{2}$. Use of Table II together with Table I allows us to obtain the selection rules for all exciton states with a given orbital symmetry. We see, for example, that the ground-state heavy-hole excitons are forbidden for light polarized along the growth direction. Moreover, ground-state excitons belonging to subbands with opposite parities, such as HH2-CB1 or LH1-CB2, have zero oscillator strength. It is important to remark that these selection rules are valid with full inclusion of valence-band mixing,[31] contrary to some statements made in the literature.[14] The effect of valence-band mixing is to give a finite oscillator strength to some excitons in excited states, such as

TABLE II. Selection rules for one- and two-photon transitions, for excitons labeled by the quantum numbers (conduction subband, value of m). The symbols x, y, z denote the polarizations of the light beam for which the transition strength does not vanish.

conduction subband	m	one photon	two photons
CB1	$\frac{3}{2}$	xy	
CB1	$\frac{1}{2}$		xy, xz, zz
CB1	$-\frac{1}{2}$	xy, z	
CB1	$-\frac{3}{2}$		xy, xz
CB2	$\frac{3}{2}$		xy, xz
CB2	$\frac{1}{2}$	xy, z	
CB2	$-\frac{1}{2}$		xy, xz, zz
CB2	$-\frac{3}{2}$	xy	

HH2-CB1 ($2p_+$) or LH1-CB2 ($2p_-$). Another property which follows from symmetry is that, for excitons with $m = \pm\frac{1}{2}$, the oscillator strength for light polarized along z is four times that for light polarized along x, y.

D. Conduction-band nonparabolicity

Conduction band (CB) nonparabolicity is included by using the anisotropic CB dispersion computed in Ref. 32 from a fit to a 14-band $\mathbf{k}\cdot\mathbf{p}$ model. Neglecting the small spin splitting, and averaging in the k_x-k_y plane in order to have an axially symmetric dispersion, we have

$$E(\mathbf{k}_\parallel, k_z) = \frac{\hbar^2}{2m^*}(\mathbf{k}_\parallel^2+k_z^2)+\alpha(\mathbf{k}_\parallel^2+k_z^2)^2+\beta(\mathbf{k}_\parallel^2 k_z^2+\tfrac{1}{8}\mathbf{k}_\parallel^4), \tag{14}$$

where the $\mathbf{k}$-dependent parameters α, β are given in Ref. 32. The in-plane dispersion of the conduction subbands is obtained from (14) by first calculating the subband energies at $\mathbf{k}_\parallel = 0$, and then considering k_z as fixed: the results are essentially equivalent to those obtained with the more elaborate method of Ref. 33. It can be seen that bulk nonparabolicity has a threefold effect.

(1) Confinement energies at $\mathbf{k}_\parallel = 0$ are determined by an energy-dependent effective mass $m_\perp = m^*/(1+\alpha 2m^* k_z^2/\hbar^2)$.

(2) The in-plane effective mass $m_\parallel = m^*/[1 + (2\alpha+\beta)2m^* k_z^2/\hbar^2]$ is different from the bulk effective mass m^* and from the perpendicular effective mass $m_\perp$.

(3) The in-plane dispersion is slightly nonparabolic.

Effect (1) changes the energies of optical transitions, but is of little importance for exciton binding energies. The important effects are (2) and (3), as the effective Rydberg is proportional to the reduced parallel effective mass. The nonparabolicity effect on $m_\parallel$ is about three times larger than on $m_\perp$: therefore, including nonparabolicity using an isotropic and energy-dependent effective mass would lead to a considerable underestimation of the effect. Our results in this respect are essentially equivalent to those of Refs. 18 and 33.

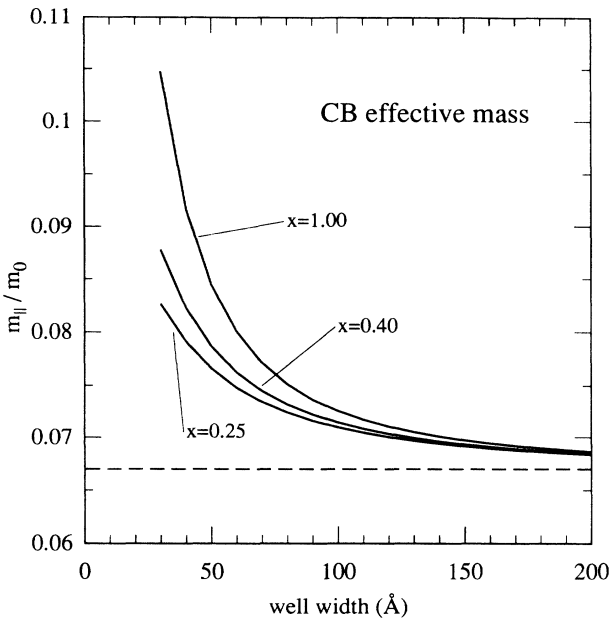

FIG. 1. In-plane effective mass of the lowest conduction subband in GaAs-$Ga_{1-x}Al_xAs$ quantum wells with different values of x, in units of the free-electron mass. The dashed line denotes the conduction-band effective mass in bulk GaAs ($m^* = 0.067 m_0$).

In Fig. 1 we show the in-plane mass $m_\parallel$ for the first conduction subbands in GaAs-$Ga_{1-x}Al_xAs$ quantum wells of different well widths and barrier heights. It can be seen that nonparabolicity considerably increases the parallel effective mass, particularly in GaAs/AlAs quantum wells. Formula (14) is quoted to be accurate for energies within 0.2 eV from the band edge. When the energy of the first conduction subband is higher than 0.2 eV, which happens in GaAs/AlAs quantum wells narrower than about 35 Å, formula (14) has only qualitative validity. The results reported in Fig. 1 are useful in order to understand the origin of the high exciton binding energies reported in the next section.

E. Dielectric mismatch

As said before, the dielectric mismatch is taken into account by considering an infinite series of image charges. We emphasize that we take into account the whole series of image charges for all possible positions of electron and hole in the well and barrier materials. In GaAs-$Ga_{1-x}Al_xAs$ QW's, this effect tends to increase the binding energy, as the dielectric constant in the barrier is smaller than in the well. It is important to remark[12] that the effect of the dielectric mismatch is a purely electrostatic one, which depends marginally on the amount of wave function in the barriers. As such, it would exist even if the barriers were infinitely high from the elec-

tronic point of view. In fact, the effect is largest for GaAs/AlAs QW's, where the barriers are higher but the dielectric mismatch is maximized.

We have neglected the contribution to the image-charge potential coming from the electron and hole self-energies.[13] The effect of these terms on the exciton binding energy vanishes for the separable wave function of Ref. 6, as the self-energy shift of electron and hole subbands exactly compensates for the shift of the exciton energy: since the separable wave function gives a good approximation to the binding energy for a well width $L \sim a_B$,[6] the self-energy effect to the exciton *binding* energy is expected to be very small. In fact, we have verified using first-order perturbation theory that the self-energy correction to the exciton binding energy is < 0.1 meV even for a 30-Å -wide GaAs/AlAs quantum well.

The effect of the dielectric mismatch can be estimated in a two-band model with a separable wave function and infinite barriers,[6] by treating the potential of the first image charge in first-order perturbation theory. This yields the following expression for the increase in binding energy:

$$\Delta E = 2\frac{\epsilon - \epsilon'}{\epsilon + \epsilon'}\frac{e^2}{\epsilon L} I(\alpha L), \tag{15}$$

where ϵ, ϵ' are the dielectric constants of well and barrier materials respectively, α is the inverse exciton radius, and where

$$I(\alpha L) = \int_0^\infty \frac{(2\alpha L)^3}{[x^2 + (2\alpha L)^2]^{3/2}} \frac{e^{-x}}{[1 + (x/2\pi)^2]^2} \times \left(\frac{\sinh(x/2)}{x/2}\right)^2 dx, \tag{16}$$

is a quantity of order unity. The energy shift depends on the well width essentially like $1/L$. For example, in a 100-Å-wide GaAs-$Ga_{0.6}Al_{0.4}As$ QW, the binding energy is expected to increase by 0.7 meV, in fair agreement with the results of the complete theory.

F. Coupling with the continuum

Coulomb coupling is included in this theory via the expansion (2) over different valence subbands. For discrete exciton states (like the ground state HH1-CB1 exciton, which is always the lowest state), coupling with discrete and continuum states belonging to other exciton series is automatically taken into account. However, an annoying difficulty arises in this theory (as in any other one which explicitly considers valence-band mixing) when an exciton state is degenerate with the continuum of other excitons. This is the case, for example, for the LH exciton in GaAs-$Ga_{1-x}Al_xAs$ QW's narrower than about 130 Å. When this happens, the discrete exciton state becomes a Fano resonance.[34] We are not aware of any first-principles treatment of excitons degenerate with the continuum. The procedure we follow here[22] corresponds to a calculation of the absorption coefficient within the variational basis. We take the variational eigenstates which happen to lie near the energy position of the resonance, and compute the average energy weighted with the oscillator strength. The oscillator strength of the resonance is defined to be the sum of the oscillator strengths of the individual states. Both quantities are seen to converge rapidly on increasing the density of variational eigenstates in the energy region of the resonance, which can be done by carefully choosing the parameters of the Gaussian trial functions (8).

This method is well suited in order to study states with a large oscillator strength, superimposed on a weak continuum background [as is the case for the LH1-CB1 (1s) exciton, which couples with the weak d_--like continuum of HH1-CB1]. It fails for states with an oscillator strength comparable to that of the continuum: however, such states will also be difficult to observe experimentally. Altogether, this procedure has the advantage of emphasizing the quantity of experimental interest, namely the absorption coefficient. Our procedure is similar to that used in Ref. 21, but we do not discretize the continuum in a larger box.

The procedure used here receives support from a study of a simple one-dimensional model,[35] where the variational solution can be compared to the exact solution and also to the results of the Fano theory. The three methods of solution are found to yield the same result for the energy shift. Furthermore, the one-dimensional model shows that the Fano width can also be obtained within the variational method.[35]

III. RESULTS FOR BINDING ENERGIES

In this section we present numerical results for exciton binding energies referring to GaAs-$Ga_{1-x}Al_xAs$ quantum wells. The band parameters used in the calculation[36] are given in Table III for GaAs and AlAs: those of $Ga_{1-x}Al_xAs$ are obtained by linear interpolation. For the band-gap difference, we take the Casey-Panish formula[37] $\Delta E_g = 1.247x$ eV for $x < 0.45$ and $\Delta E_g = 1.247x + 1.147(x-0.45)^2$ eV for $0.45 < x < 1$. The valence-band offset is taken to be 35% of the total band-gap difference.

In Fig. 2 we show the binding energy of the ground-state heavy-hole exciton in GaAs-$Ga_{0.6}Al_{0.4}As$ quantum wells of various widths, as a function of the approximations used in the calculation; in Fig. 3 we present similar results for the ground-state light-hole exciton. The dotted lines represent the results obtained by keeping only one conduction and one valence subband *(two-band*

TABLE III. Material parameters.

parameter	GaAs	AlAs
m^*	0.067	0.15
γ_1	6.85	3.45
γ_2	2.10	0.68
γ_3	2.90	1.29
ϵ	12.53	10.06
$2\lvert\langle u_c\rvert \mathbf{p} \rvert u_v\rangle\rvert^2/m_0$	25.7 eV	25.7 eV

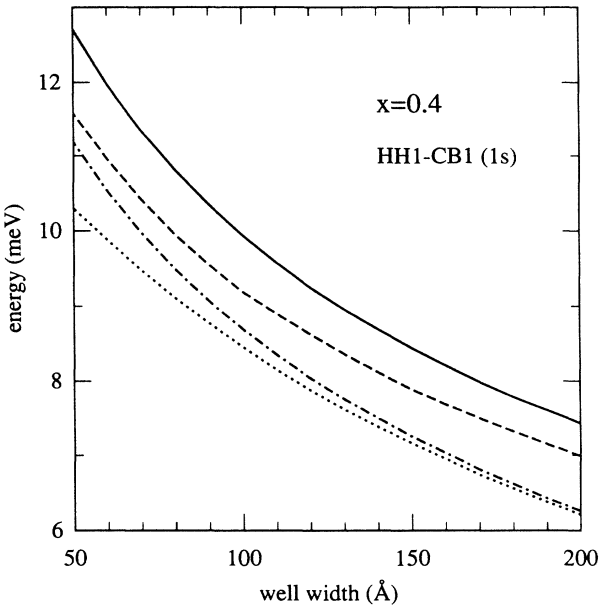

FIG. 2. Binding energy of the ground-state HH1-CB1 exciton in GaAs-$Ga_{0.6}Al_{0.4}As$ quantum wells. Dashed line: two-band approximation, parabolic CB, equal dielectric constants. Dashed-dotted line: including CB nonparabolicity. Dashed line: including nonparabolicity and Coulomb coupling. Solid line: full calculation, including also the dielectric mismatch.

approximation), with a parabolic conduction-band, and taking the dielectric constant of $Ga_{1-x}Al_xAs$ to be the same as for GaAs. The dashed-dotted line is calculated including conduction band nonparabolicity. The dashed line includes also the effect of Coulomb coupling, besides that of nonparabolicity. The solid line includes also the dielectric mismatch, and therefore represents the full calculation. All three effects are seen to increase the binding energy by comparable amounts, particularly for narrow wells. Nonparabolicity is negligible for large wells, but becomes rapidly important for narrow wells. The effect of Coulomb coupling grows for thicker wells, as the subband separation becomes smaller, and is particularly important for the light-hole exciton, where it increases the binding energy by more than 2 meV. For the HH1-CB1 ($1s$) exciton, only coupling to LH1-CB1 is kept, as the remaining subbands give a contribution of the order of 0.1 meV; for the LH1-CB1 ($1s$) exciton, instead, it is necessary to include coupling to both HH1-CB1 and HH2-CB1. It should be remarked that coupling is mainly with the *continuum* of other exciton series, and is in fact much larger than found in Ref. 20, where coupling with the continuum was neglected. The effect of the dielectric mismatch is seen to be large, similar for both excitons, and to decrease slowly with the well width according to the approximate formula (15).

In Figs. 4 and 5 we present the binding energies of the ground-state heavy- and light-hole excitons for the full calculation, for three different values of the aluminum concentration. The case $x = 1$ refers to AlAs barriers: the crossover from direct to indirect gap, which takes place at a well width of about 35 Å,[26] should not change the results reported in Figs. 4 and 5 (even if the lowest exciton becomes indirect), as the effect of Γ-X mixing is small.[24] It can be seen that the binding energy of the ground-state HH and LH excitons depends very markedly on the aluminum concentration. It is important to observe that this dependence is *not* an effect of confinement, as the exciton is already largely confined within the well.

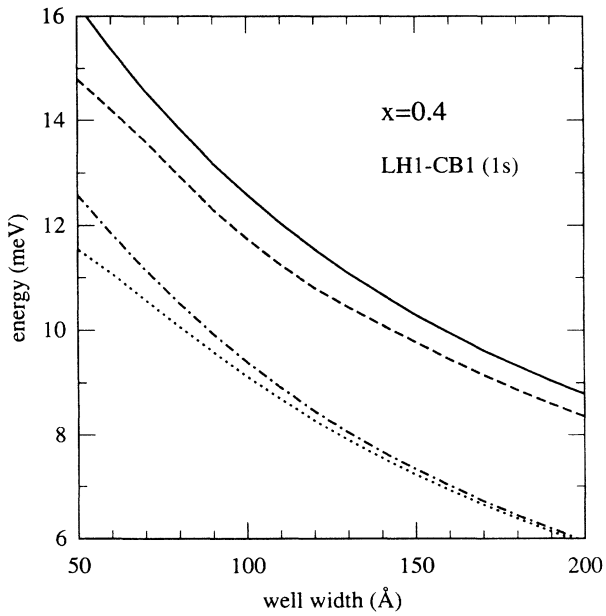

FIG. 3. Binding energy of the ground-state LH1-CB1 exciton in GaAs-$Ga_{0.6}Al_{0.4}As$ quantum wells. The meaning of the different curves is the same as in Fig. 2.

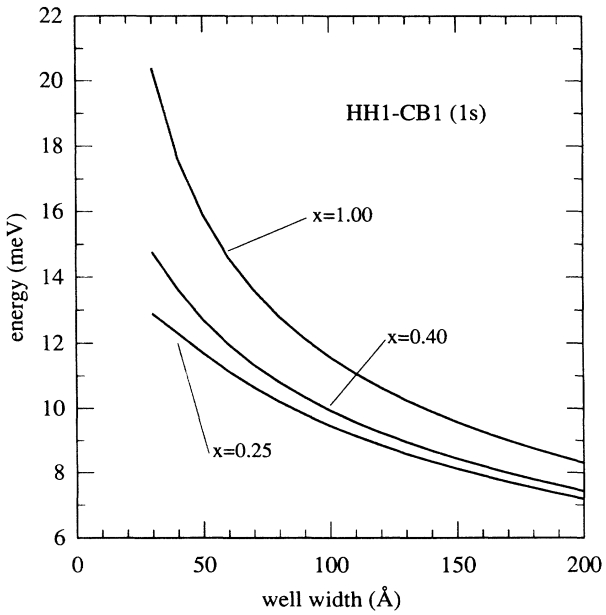

FIG. 4. Binding energy of the ground-state HH1-CB1 exciton in GaAs-$Ga_{1-x}Al_xAs$ quantum wells for different values of x.

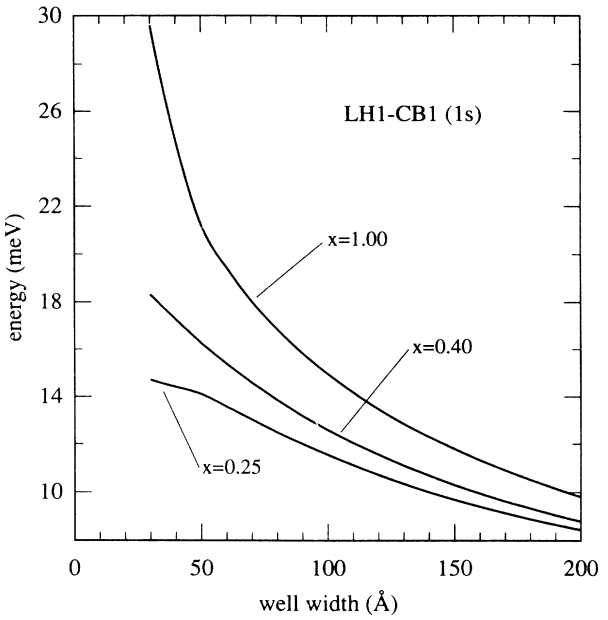

FIG. 5. Binding energy of the ground-state LH1-CB1 exciton in GaAs-$Ga_{1-x}Al_xAs$ quantum wells for different values of x.

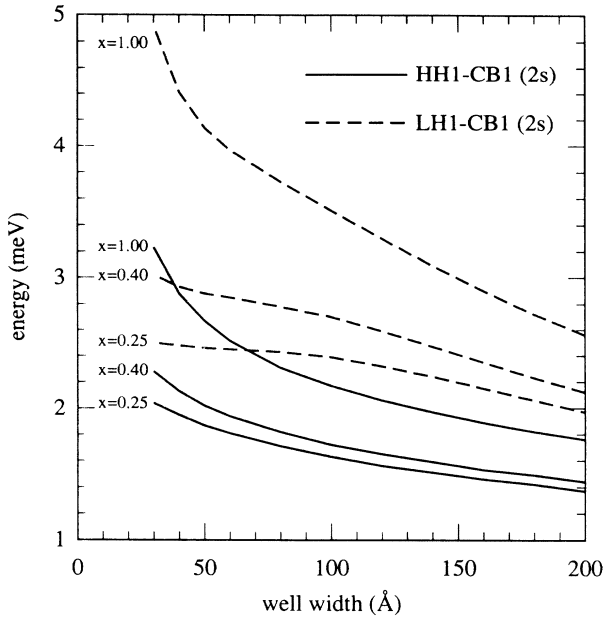

FIG. 6. Binding energies of the $2s$ states of the HH1-CB1 and LH1-CB1 excitons in GaAs-$Ga_{1-x}Al_xAs$ quantum wells for different values of x.

Rather, it is a result of conduction-band nonparabolicity (which acts via the parallel effective masses shown in Fig. 1) and the dielectric mismatch, which is obviously largest for AlAs barriers. The change in band parameters is also responsible for the fact that the binding energy can become higher than the two-dimensional limit $E_{2D} = 4E_{3D}$, i.e., about 17 meV. The high binding energies for narrow GaAs/AlAs quantum wells are therefore a peculiar result of the present theory.

In Fig. 6 we show the binding energies of the $2s$ excited states of the HH1-CB1 and LH1-CB1 excitons for three different aluminum concentrations. For simplicity, the two-band approximation has been adopted, which for the $2s$ states imply an error smaller than 0.2 meV.[22] The energies of the $2s$ states follow similar trends as the corresponding $1s$ states, on a reduced energy scale. They can be much larger than reported in the literature,[7,20,21] particularly for the light-hole exciton. Here, again, the dependence on the concentration comes mainly from nonparabolicity and the dielectric mismatch.

The work of Ref. 7 first called attention to the fact that the exciton binding energy should reach a maximum at a critical well width, when the exciton wave function starts to spread into the barriers. We have found no evidence for a decrease in binding energy in the range of well widths we have studied. This is due in part to the fact that we have considered higher aluminum concentrations than in Ref. 7, and in part to conduction-band nonparabolicity and the dielectric mismatch, whose effect grows for narrow wells and tends to push the critical width down to smaller values. Our expansion set is clearly not adequate in the limit $L \rightarrow 0$ (apart from the fact that the effective-mass approximation itself breaks down), as the contribution of the subband continuum can no longer be neglected: however, the subband continuum is not expected to be important before the first conduction level is within a few exciton binding energies from the top of the well, which is never the case for $L > 30$ Å. The conclusion which follows from our calculation is that the expected decrease in exciton binding energy does not occur for $L > 30$ Å and $x > 0.25$.

The most reliable measurements of the exciton binding energy come from photoluminescence excitation (PLE) experiments in high-quality samples, where the $2s$ state is seen as a well-defined peak. In Table IV we compare some experimentally measured values[11,38,39] of the difference $E_b(1s) - E_b(2s)$ with our theoretical predictions. Agreement is at the level of 0.5 meV in the whole range of well widths. Comparison with other experiments[40] leads to similar conclusions. In particular, the underestimation of binding energies noted in Ref. 21 is resolved by the inclusion of nonparabolicity and the dielectric mismatch. Note that the binding energy is considerably higher in the GaAs/AlAs QW with $L = 82$ Å, and still in agreement with theory: according to the above discussion, this can be taken as an indication for the effect of the dielectric mismatch. Unfortunately, we are not aware of any other PLE data on GaAs/AlAs quantum wells.

Magneto-optical data are less straightforward to analyze, as the determination of the continuum edge requires using a model in order to extrapolate the experimental data to zero field. When we compare our theoretical predictions with the results of magneto-optical experiments[41–44] we find larger discrepancies ($\sim$ 1-2 meV), which, however, are not systematic. Considering the excellent agreement with PLE experiments, we

TABLE IV. Comparison of theoretically calculated values of the energy difference $\Delta E_b = E_b(1s) - E_b(2s)$ with PLE experiments, for excitons associated with the first conduction subband. Energies are in meV.

L (Å)	x	hole	theory	expt.
75	0.40	HH1	9.2	9.5[a]
		LH1	11.1	10.3[a]
82	1.00	HH1	10.3	10.9[a]
		LH1	12.7	12.5[a]
92	0.35	HH1	8.3	8.5[a]
		LH1	9.9	10.2[a]
112	0.35	LH1	9.0	9.1[a]
225	0.35	HH1	5.5	6.0[b]
		HH1	6.3[c]	6.5[b,c]
		LH1	6.0	6.2[b]
		LH1	7.0[c]	7.3[b,c]
76	0.33	HH1	8.9	8.6[d]
71	0.33	HH1	9.1	8.6[d]

[a] Reference 11.
[b] Reference 38.
[c] $E_b(1s) - E_b(3s)$.
[d] Reference 39.

are led to conclude that the models used in analyzing magneto-optical data still have some uncertainty.

No other serious sources of error should affect theoretical predictions. Convergence is under control, the effect of nonaxial terms is very small,[21] and the dynamical polaronic effect[45] has about the same size (~ 0.2 meV) as in the bulk. Effects of spatially dependent screening should be slightly smaller than for donors, where they increase the binding energy by ~ 0.3 meV in a QW with $L = 50$ Å and infinite barrier height.[46] Effects of the exchange interaction are calculated to be small, except for the z-polarized light-hole exciton, which is shifted upwards by a non-negligible amount.[47,48] For wells narrower than about 50 Å, and for the highest values of x, corrections are likely to arise from a renormalization of material parameters and (which is actually the same thing) from the way in which nonparabolicity is taken into account. For wider wells ($L > 300$ Å), Coulomb coupling with higher subbands becomes essential, and the physics gradually changes from a regime dominated by quantization of the subbands to a regime characterized by quantization of the center-of-mass motion of the exciton.[49]

IV. OSCILLATOR STRENGTH

The study of oscillator strengths of quantum-well excitons has two aspects. The first is an accurate evaluation of the oscillator strength of the dominant transitions, particularly the ground-state HH and LH excitons. The second is the effect of valence-band mixing on the oscillator strength of otherwise forbidden transitions and the validity of the selection rules derived in Sec. II. This second aspect has been treated in detail in Refs. 20 and 22 and will not be repeated here. There is now mounting evidence for the validity of the parity selection rule: observation of ground-state excitons such as HH2-CB1 or LH1-CB2 is possible only when an electric field is present in the sample,[50] otherwise these excitons can only be observed in p-like excited states.[39]

In Fig. 7 we show the oscillator strength per unit area for in-plane polarization of the ground-state heavy- and light-hole excitons in GaAs-$Ga_{0.6}Al_{0.4}As$ quantum wells of various widths. Nonparabolicity and the dielectric mismatch have a negligible effect on the oscillator strengths, which also depend little on the aluminum concentration in the barriers. The ratio of the oscillator strengths of heavy- to light-hole exciton, which would be 3 in the absence of valence-band mixing, becomes about 2 when valence-band mixing is included. It has been shown in Ref. 22 that inclusion of Coulomb coupling is essential in order to obtain not only the correct values, but also the correct ratio for the oscillator strengths. Concerning the dependence on the well width, the oscillator strengths calculated here grow more rapidly than calculated in Ref. 21 as the well width is reduced. We do not know the reason for this discrepancy.

Also shown in Fig. 7 are experimentally measured values for the oscillator strengths.[51,52] The values of Ref. 51 (taken on GaAs/$Ga_{0.75}Al_{0.25}As$ quantum wells) were directly obtained from absorption measurements. In order to obtain the oscillator strength from the reflectivity data of Ref. 52 (taken on GaAs/$Ga_{0.7}Al_{0.3}As$ quantum wells) it is necessary to calculate the reflectivity from a quantum well within a microscopic approach which re-

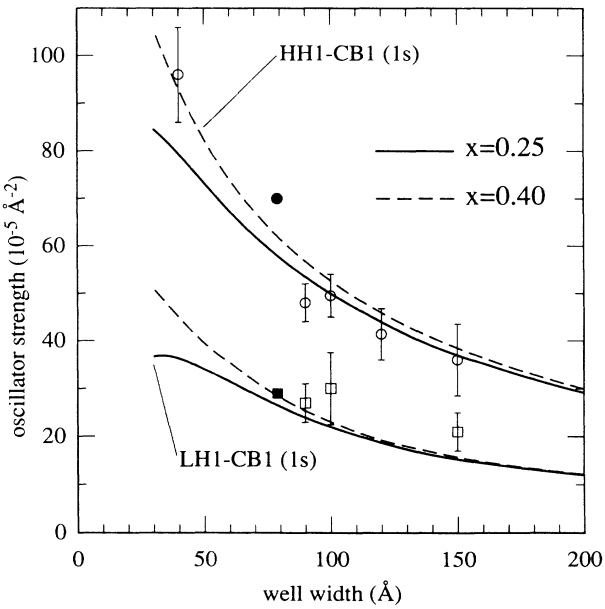

FIG. 7. Oscillator strength per unit area for in-plane polarization for the ground-state HH1-CB1 and LH1-CB1 excitons in GaAs-$Ga_{1-x}Al_xAs$ QW's of varying width. Experimental points: circles, HH exciton; squares, LH exciton; open symbols, Ref. 51 (with $x = 0.25$); solid symbols, Ref. 52 (with $x = 0.30$).

lates the oscillator strength per unit area to experimentally measured parameters. Such a calculation, which will be the subject of a subsequent publication,[53] shows that the relation between the parameter A defined in Ref. 52 and the oscillator strength per unit area $\tilde{f}$ is $\tilde{f} = (m_0 LA)/(4\pi\hbar^2 e^2)$. This relation was used in order to obtain the data reported in Fig. 7. Experiment and theory are in reasonable agreement, and this agreement can only be obtained if Coulomb coupling is included. For $L > 200$ Å, the accuracy of the calculation is expected to deteriorate rapidly, as the oscillator strength is very sensitive to coupling to higher subbands.

V. CONCLUSIONS

Exciton binding energies have been calculated including valence-band mixing and also other important effects, namely Coulomb coupling between excitons associated to different valence subbands, nonparabolicity of the bulk conduction band, and the difference in dielectric constants between GaAs and $Ga_{1-x}Al_xAs$. Coupling with other exciton series is predominantly with the exciton continuum. Binding energies are predicted to increase monotonically as the well width is reduced for $L > 30$ Å and $x > 0.25$.

The effects of Coulomb coupling, nonparabolicity, and the dielectric mismatch are of similar importance, go in the direction of increasing the binding energy, and taken together result in much higher binding energies than previously suspected. This is true for the ground state as well as for the excited states. Binding energies can be even higher than the two-dimensional limit $E_{2D} = 4E_{3D}$, due to the change in the conduction-band effective mass and in the dielectric constant. In particular, the effect of the dielectric mismatch does not depend on the amount of the exciton wave function in the barriers, but rather on the strength and the position of the first image charges: therefore it is particularly sizeable in GaAs/AlAs quantum wells. Calculated binding energies agree at the level of 0.5 meV with photoluminescence excitation data which measure the $1s$-$2s$ splitting. It would be interesting to have more data on narrow (~30–70-Å-wide) GaAs/AlAs quantum wells, where the effect of the dielectric mismatch is largest and where the present theory mostly differs from existing ones. The high binding energy of the exciton in GaAs/AlAs QW's (where the barriers can also be AlAs/GaAs superlattices) might be of importance for the stability of the exciton, also in view of device applications.

It is interesting to pose the question as to which extent the results obtained in this paper for GaAs-$Ga_{1-x}Al_xAs$ QW's remain qualitatively valid for other III-V materials. The effect of Coulomb coupling always goes in the direction of increasing the binding energy for the lowest exciton state, which is coupled to higher-lying states. For the light-hole exciton, however, the sign of the effect cannot be predicted by simple arguments. The effect of CB nonparabolicity should generally go in the direction of increasing the binding energy, as the increase of the CB effective mass for energies above the band edge is a common feature of direct-gap III-V semiconductors. This effect should be larger in materials with smaller gap, as for the InAs/GaSb quantum well. The effect of the dielectric mismatch depends on the relative size of the dielectric constants in the well and barrier materials. A thorough investigation of this effect for several materials has been given in Ref. 13.

Concerning the oscillator strengths, valence-band mixing is found to have both a quantitative effect (as evidenced for example from the ratio of the oscillator strengths of HH1-CB1 to LH1-CB1) and a qualitative effect, as some excitons become allowed in excited states. However, valence-band mixing does not change selection rules based on parity and polarization properties. Calculated oscillator strengths of the ground-state heavy- and light-hole excitons agree well with absorption and reflectivity measurements.

ACKNOWLEDGMENTS

We are grateful to F. Bassani for his continuous encouragement. We acknowledge useful and stimulating discussions with A. Baldereschi, G. Bastard, R. Buczko, R. Del Sole, R. Elliott, and S. Fraizzoli. One of the authors (L.C.A.) wishes to acknowledge partial support from the Swiss National Science Foundation under Grant No. 20-5446.87.

[1] R. Dingle, W. Wiegmann, and C. H. Henry, Phys. Rev. Lett. **33**, 827 (1974).
[2] R. Dingle, in *Festkörperprobleme XV*, edited by H. J. Queisser (Vieweg, Braunschweig, 1975), p. 21.
[3] See, e.g., *Excitons in Confined Systems*, edited by R. Del Sole, A. D'Andrea, and A. Lapiccirella (Springer, Berlin, 1988), and references therein.
[4] C. Weisbuch, R. C. Miller, R. Dingle, A. C. Gossard, and W. Wiegmann, Solid State Commun. **37**, 219 (1981).
[5] R. C. Miller, D. A. Kleinman, W. T. Tsang, and A. C. Gossard, Phys. Rev. B **24**, 1134 (1981).
[6] G. Bastard, E. E. Mendez, L. L. Chang, and L. Esaki, Phys. Rev. B **26**, 1974 (1982).
[7] R. L. Greene, K. K. Bajaj, and D. E. Phelps, Phys. Rev. B **29**, 1807 (1984).
[8] Y.-C. Chang and J. N. Schulman, Appl. Phys. Lett. **43**, 536 (1983).
[9] M. Altarelli, U. Ekenberg, and A. Fasolino, Phys. Rev. B **32**, 5138 (1985).
[10] M. Matsuura and Y. Shinozuka, J. Phys. Soc. Jpn. **53**, 3138 (1984).
[11] P. Dawson, K. J. Moore, G. Duggan, H. I. Ralph, and C.

T. B. Foxon, Phys. Rev. B **34**, 6007 (1986).
[12]D. M. Whittaker and R. J. Elliott, Solid State Commun. **68**, 1 (1988).
[13]M. Kumagai and T. Takagahara, Phys. Rev. B **40**, 12 359 (1989).
[14]G. D. Sanders and Y.-C. Chang, Phys. Rev. B **32**, 5517 (1985); **35**, 1300 (1987).
[15]K. S. Chan, J. Phys. C **19**, L125 (1986).
[16]D. A. Broido and L. J. Sham, Phys. Rev. B **34**, 3917 (1986).
[17]S.-R. E. Yang and L. J. Sham, Phys. Rev. Lett. **58**, 2598 (1987).
[18]U. Ekenberg and M. Altarelli, Phys. Rev. B **35**, 7585 (1987).
[19]T. Hiroshima, Phys. Rev. B **36**, 4518 (1987).
[20]B. Zhu and K. Huang, Phys. Rev. B **36**, 8102 (1987); B. Zhu, *ibid.* **37**, 4689 (1988).
[21]G. E. W. Bauer and T. Ando, Phys. Rev. B **38**, 6015 (1988).
[22]L. C. Andreani and A. Pasquarello, Europhys. Lett. **6**, 259 (1988); Superlatt. Microstruct. **5**, 59 (1989).
[23]For a review, see, e.g., M. Altarelli, in *Heterojunctions and Semiconductor Superlattices*, edited by G. Allan, G. Bastard N. Boccara, M. Lannoo, and M. Voos (Springer, Berlin, 1986); G. Bastard, and J. A. Brum, IEEE J. Quantum Electron. **QE-22**, 1625 (1986).
[24]T. Ando, S. Wakahara, and H. Akera, Phys. Rev. B **40**, 11 609 (1989).
[25]C. Priester, G. Allan, and M. Lannoo, Phys. Rev. B **28**, 7194 (1983).
[26]K. J. Moore, G. Duggan, P. Dawson, and C. T. Foxon, Phys. Rev. B **38**, 5535 (1988).
[27]J. M. Luttinger and W. Kohn, Phys. Rev. **97**, 869 (1955).
[28]A. Pasquarello, L. C. Andreani, and R. Buczko, Phys. Rev. B **40**, 5602 (1989).
[29]L. C. Andreani, A. Pasquarello, and F. Bassani, Phys. Rev. B **36**, 5887 (1987).
[30]S. Fraizzoli, F. Bassani, and R. Buczko, Phys. Rev. B **41**, 5096 (1990).
[31]For a symmetry analysis, see L. C. Andreani, F. Bassani, and A. Pasquarello, in *Symmetry in Nature*, edited by G. Bernardini (Quaderni della Scuola Normale Superiore, Pisa, 1989), p. 19. See also L. C. Andreani, PhD. thesis, Scuola Normale Superiore, Pisa, 1989 (unpublished).
[32]U. Rössler, Solid State Commun. **49**, 943 (1984).
[33]U. Ekenberg, Phys. Rev. B **40**, 7714 (1989).
[34]U. Fano, Phys. Rev. **124**, 1866 (1961).
[35]A. Pasquarello and L. C. Andreani (unpublished).
[36]*Landolt-Börnstein Numerical Data and Functional Relationships in Science and Technology*, edited by O. Madelung (Springer, Berlin, 1982), Group III, Band 17.
[37]H. C. Casey and M. B. Panish, *Heterostructure Lasers* (Academic, New York, 1978), part A.
[38]D. C. Reynolds, K. K. Bajai, C. Leak, G. Peters, W. Theis, P. W. Yu, K. Alavi, C. Colvard, and I. Shidlovsky, Phys. Rev. B **37**, 3117 (1988).
[39]L. W. Molenkamp, G. E. W. Bauer, R. Eppenga, and C. T. Foxon, Phys. Rev. B **38**, 6147 (1988).
[40]E. S. Koteles and J. Y. Chi, Phys. Rev. B **37**, 6332 (1988).
[41]D. C. Rogers, J. Singleton, R. J. Nicholas, C. T. Foxon, and K. Woodbridge, Phys. Rev. B **34**, 4002 (1986).
[42]A. S. Plaut, J. Singleton, R. J. Nicholas, R. T. Harley, S. R. Andrews, and C. T. B. Foxon, Phys. Rev. B **38**, 1323 (1988).
[43]M. Dutta, X. Liu, A. Petrou, D. D. Smith, M. Taysing-Lara, and L. Poli, Superlatt. Microstruct. **4**, 147 (1988).
[44]D. D. Smith, M. Dutta, X. C. Liu, A. F. Terzis, A. Petrou, M. W. Cole, and P. G. Newman, Phys. Rev. B **40**, 1407 (1989).
[45]M. Matsuura, Phys. Rev. B **37**, 6977 (1988).
[46]L. E. Oliveira and L. M. Falicov, Phys. Rev. B **34**, 8676 (1986).
[47]Y. Chen, B. Gil, P. Lefebvre, and H. Mathieu, Phys. Rev. B **37**, 6429 (1988).
[48]L. C. Andreani and F. Bassani, Phys. Rev. B **41**, 7536 (1990).
[49]A. D'Andrea, R. Del Sole, and K. Cho, Europhys. Lett. **11**, 169 (1990).
[50]L. Viña, Surf. Sci. **196**, 569 (1988).
[51]W. T. Masselink, P. J. Pearah, J. Klem, C. K. Peng, H. Morkoç, G. D. Sanders, and Y.-C. Chang, Phys. Rev. B **32**, 8027 (1985).
[52]B. Gil, Y. El Khalifi, H. Mathieu, C. de Paris, J. Massies, G. Neu, T. Fukunaga, and H. Nakashima, Phys. Rev. B **41**, 2885 (1990).
[53]L. C. Andreani, F. Tassone, and F. Bassani, unpublished.